

Band aggregators for band-unaware multi-band CDC-ROADM

Kenya Suzuki^{1*} and Mitsunori Fukutoku²

¹NTT Device Innovation Center, NTT Corporation, 3-1 Morinosato Wakamiya, Atsugi, Kanagawa 243-0198, Japan

²NTT Innovative Devices Corporation, 1-1-32 Shin Urushima, Yokohama, Kanagawa 221-0031, Japan

Author e-mail address: kny.suzuki@ntt.com

Abstract: We report on the concept of a multi-band CDC-ROADM network without network operators being aware of the differences between bands and its enabling devices, i.e., band aggregators. © 2024 The Author(s)

1. Introduction

In optical line systems, the signal bit rate and its occupation in bandwidth have drastically increased in recent years [1]. This is partly due to the increase in the bit rate of client signals driven by the demands of the 5G mobile and remote work environment. To accommodate these client signals efficiently and transmit the aggregated signals over long distances, it is essential to relax the multilevel format and maximize the baud rate of signals. However, this trend causes a reduction in the number of signals in the wavelength division multiplexing (WDM) wavelength band. For example, a WDM system with a 100-Gbps and 50-GHz channel spacing can accommodate almost 100 signals in the C-band; however, an 800-Gbps and 150-GHz spacing system can accommodate only 32 signals in the C-band. The decrease in the number of channels impacts insufficient optical path establishments in a complex optical network. More seriously, the transmission capacity per fiber does not increase even though the bit rate per signal expands. Countermeasures against the aforementioned issue include utilizing space-division-multiplexing (SDM) [2–4] and multi-band transmission systems where S/C/L bands coexist [4–6]. The former appears essential because it may provide an infinite total bandwidth increase; however, from an economic viewpoint, the SDM system requires the investment of additional or new optical fiber. On the other hand, multi-band systems can reuse the installed optical fibers by adding or replacing node equipment, resulting in less investment. The multi-band systems that share the same fibers and node equipment with different bands reap the benefits of the divide-and-conquer effect. Numerous studies have been reported regarding the multi-band systems, including economics [7], transmission [8, 9], network provisioning [10, 11], architecture [12, 13], and devices [14–17]. In this report, we propose a concept of a band-unaware, color-less, direction-less, and contention-less reconfigurable optical add/drop multiplexing (CDC-ROADM) node, and its enabling switching devices, i.e., band aggregators that offer a simple operation of a multi-band network.

2. Band-unaware multi-band CDC-ROADM

As described in the previous section and in previous reports, multi-band systems are advantageous to increase the capacity per fiber. However, it is operationally beneficial to be able to treat the multiple bands as a single band. In other words, it is preferable to simplify the operation and treat multiple bands as one band rather than as different bands from the network provider's viewpoint. To handle these multiple bands as one, the elements of the network system, such as operating software, equipment and devices, must be able to accommodate and conceal the complexities arising from multi-band operation. These devices include multi-band tunable transponders, multi-band optical amplifiers, and multi-band optical switches. Among these, the multi-band operation of transponders and amplifiers appears to be difficult at this point due to the bandwidth limitation of the gain medium for diode lasers and rare-earth material. On the other hand, with regard to switch devices such as wavelength-selective switches and transponder aggregators (TPA: multicast switches [18, 19] or $M \times N$ wavelength-selective switches (WSSs) [20, 21]), they are

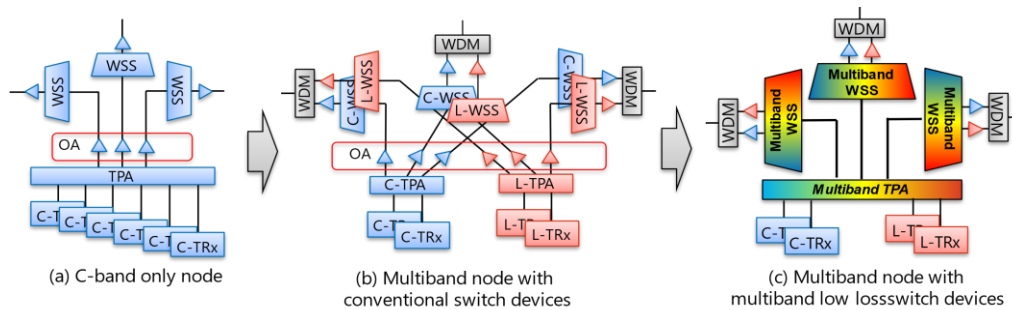


Fig. 1. Schematic diagram of CDC-ROADM node for (a) single band, (b) multi-band with conventional single band devices, and (c) multi-band with multi-band devices.

uncomplicated to make the switch operate multi-band because they are passive devices and have small physical restrictions. The usage of these multi-band switch devices offers significant advantages in terms of both node configuration and operation [22]. Figure 1 shows the evolution of CDC-ROADM node configuration [18–23]. When transitioning from a single-band system (Fig. 1 (a)) to a multi-band system, if we use band-specific switch devices (Fig. 1 (b)), the node configuration becomes complex. In contrast, multi-band switches (Fig. 1 (c)) simplify the node configuration as well as node operation. When an operator installs additional transponders in the system, they must ensure they plug the correct transponder into the correct port if the TPAs are band-specific. Mistakes may interfere with plans to expand transmission capacity. A system with multi-band switches also operating as a *band aggregator* does not need to be aware of which system it is connecting to, improving its operability. A possible drawback of using multi-band multicast switches (MCSs) is that we need additional C/L-band WDM couplers when we install an optical amplifier to compensate for the loss of the node [not shown in Fig. 3(c)]. Thus, reducing the insertion loss of the TPAs is essential to develop a simple node to avoid the unbundling of different bands [23].

3. Band aggregation switches for band-unaware multi-band CDC-ROADM

3.1. Multi-band multicast switches

As a TPA, MCSs are widely deployed in real network systems [18]. The MCSs are composed of silica-based planar lightwave circuits (PLC) [24] or micro electro-mechanical systems (MEMS) [25] as their technology. Silica-based PLCs have demonstrated excellent optical characteristics, mechanical stability, and high reliability. The switching mechanism is based on Mach-Zehnder interferometer (MZI) switches that exhibited wavelength dependence. Recently, the multi-band operation of the MZI was reported over the O to L band [26]. Combining it with a wavelength-independent coupler [27] provides wideband operation for MCSs. Figure 2 shows the transmission characteristics of a recently fabricated multi-band 16-degree/8-transponder MCS. The excess loss was less than 3 dB over the S to L band, and sufficient extinction of more than 40 dB was obtained.

3.2. Multi-band transponder aggregator with filtering function

Another alternative for TPA is the $M \times N$ WSS, which can handle M degrees and N transponders [20, 21]. The $M \times N$ WSS consists of M sets of $1 \times N$ WSSs and N sets of $M \times 1$ non-wavelength-selective switches. It provides low-loss characteristics, even when the number of transponder ports becomes large, whereas the MCS increases its principle loss as the transponder port count. The noise filtering function is another feature of $M \times N$ WSS. When WDM signals are transmitted through a transmission line, the optical noise generated by transponders at different wavelengths can degrade the signal quality, and this effect is more pronounced as the number of signals increases. To address this issue, an optical filter (bandpass filter) should be inserted just after the transmitter to reduce amplified spontaneous emission (ASE) noise. The $M \times N$ WSS includes this filtering function internally. However, one of the problems of the $M \times N$ WSS is that its scalability is limited by the area of commercially available liquid crystal on silicon (LCOS). The scalability of the $M \times N$ WSS can be quantified using the following formula [20]

$$M \times N \propto H \cdot \theta_{max} \quad (3)$$

where H is the area or height of the LCOS panel and θ_{max} is the deflection angle achievable by the LCOS. Therefore, if we extend the operating band of the $M \times N$ WSS to multiple bands, the port count (M or N) can be reduced by the number of bands. We have proposed a novel implementation of a noise-suppressing filter for the TPA by combining a commercially available multi-band WSS [16] with silica-PLC-based non-wavelength-selective switches [28]. Figure 3 (a) shows the schematic diagram. It assumes that not all of the signals need to go through the noise-suppressing filters as described below. If signals from the transponders require filtering, they are sent to the $N \times 1$ WSS, then multiplexed and routed to the designated degree by the $L \times M$ matrix switch integrated into the silica-based PLC (path α). In contrast, if signals do not need filtering, they are directly routed to the degree port by $(M+L) \times 1$ non-wavelength-selective switches (path β). This configuration offers two advantages. One is that already commercially

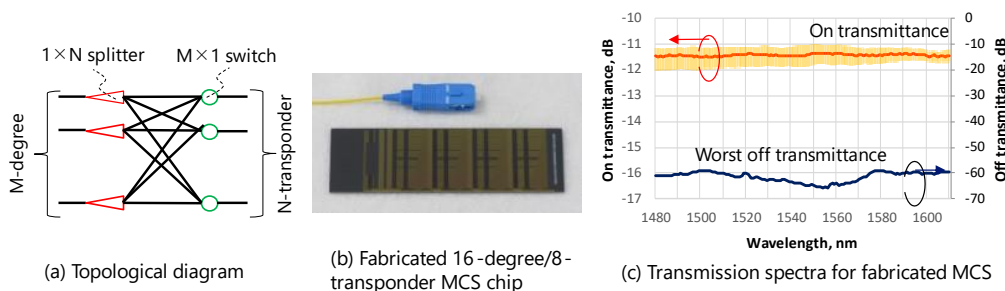
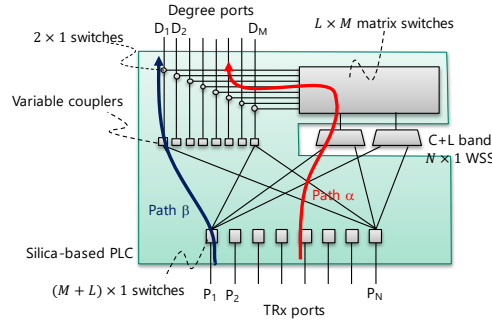
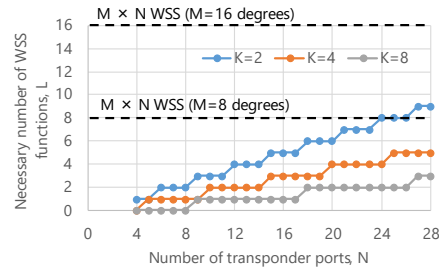


Fig. 2. Fabricated 16-degree/8-transponder MCS by silica-based PLC. (a) Topological diagram, (b) fabricated MCS chip, and (c) transmission spectra of the fabricated MCS, yellow band indicates error bar for 16×8 path combination.



(a) Schematic diagram of proposed multiband TPA with filtering function



(b) Required number of filtering functions of proposed TPA

Fig. 3. Novel multi-band transponder aggregator with filtering function. (a) Schematic and (b) the required number of filtering functions

available C+L band $1 \times N$ WSSs provide the multi-band filtering function. The other is that while an $M \times N$ WSS requires the same number of $1 \times N$ WSSs as the degree count, our proposal needs the number of $L = \text{Int}\left(\frac{N}{K+1}\right)$ of filtering function, if we can tolerate the noise superpositions of $K-1$ signals from out-of-band transponders. This can be clarified by considering a case when only one signal from a transponder is routed to a degree. In such a case, the signal does not need protection from out-of-band noise through filtering. Thus, the number of filtering functions can be reduced. In other words, an $M \times N$ WSS has $1 \times N$ WSSs that are not used as noise filters. Figure 3 (b) shows the dependence of the required number of filtering (WSS) functions on the transponder port count. As shown, if we admit noises from three signals ($K=4$) to be superimposed, for example, only four sets of filtering functions are needed, regardless of the degree port count.

3.3. Transmission experiment for band-unaware multi-band CDC-ROADM

Finally, we also conducted transmission experiments on the band-unaware multi-band CDC-ROADM using the band aggregation switches previously described. Concerning the multi-band MCS, we constructed a C+L-band node setup and transmitted a 1-Tbps signal (DP-32QAM, 66Gbaud, two-subcarrier) in the C and L bands. We confirmed that the Q-margins over the forward error correction (FEC) threshold exceeded 0.3 dB for a 2-span link [22]. For the transponder aggregator with a filtering function, we verified its applicability by introducing C-band and L-band 400 Gbps signals (DP-16QAM, 66 Gbaud). We observed that the filtering function was effective, and there was no degradation resulting from the use of the proposed transponder aggregator [28].

4. Summary

We discussed the band-unaware multi-band CDC-ROADM, which offers significant advantages in terms of network operation. Band unawareness is driven by the multi-band operable transponder aggregator or *band aggregators*. We also reported two implementations of band aggregators, i.e., the multi-band multicast switches and the combination of multi-band $1 \times N$ WSS and silica-based PLC integrated non-wavelength-selective switches.

Acknowledgement

The author is grateful to Drs. S. Camatel and Y. Ma of Finisar Australia, D. Ogawa of NTT Innovative Device Corp, and other collaborators in NTT Laboratories for their support and fruitful discussions.

References

- [1] M. Nakamura, *et al.*, *Proc. ECOC22, paper Th3C.1*. (2022)
- [2] T. Morioka, OECC09, FT4, (2009)
- [3] B. J. Puttnam, *Optica* 8, 1186–1203 (2021)
- [4] A. Ferrari, *et al.*, *J. Lightw. Technol.* 38, 1041–1049 (2020)
- [5] K. Seno, *et al.*, *IEEE J. Lightw. Technol.* 40, 1764–1775 (2022)
- [6] S. Okamoto, *et al.*, in *Proc. ECOC16* (2016)
- [7] M. Nakagawa, *et al.*, in *Proc. OFC22, W2A.24*. (2022)
- [8] F. Hamaoka, *et al.*, in *Proc. OFC23, Th3F.2*. (2023)
- [9] K. Saito, *et al.*, in *Proc. OECC23*, (2023)
- [10] N. E. D. E. Sheikh, *et al.*, ONDM21 (2021)
- [11] B. Correia, *et al.*, *J. Opt. Commun. Netw.* 13, 147–157 (2021)
- [12] J. F. Ó. Ramos, *et al.*, *Proc. ICTON23, Th.A4.5* (2023)
- [13] H. Hasegawa, *IEICE Trans. Commun. in Press*
- [14] R. Kraemer, *et al.*, *J. Lightw. Technol.*, 39, 6023–6032, (2021)
- [15] K. Seno, *et al.*, ECOC18, 1–3 (2018)
- [16] <https://www.globenewswire.com/news-release/2020/08/31/2086099/0/en/Finisar-Australia-Releases-World-s-First-C-L-band-Wavelength-Selective-Switch.html>
- [17] Ning Deng, *et al.*, *J. Lightw. Technol.* 40, 3385–3394 (2022)
- [18] T. Watanabe, *et al.*, in *Proc. OFC11*, paper OTuD3 (2021)
- [19] W. I. Way, *et al.*, in *Proc. OFC12*, paper NW3F.5. (2022)
- [20] Y. Ikuma, *et al.*, *J. Lightw. Technol.*, 34, 67–72 (2016)
- [21] P. D. Colbourne, *et al.*, in *Proc. OFC18*, pp. 1–3 (2018)
- [22] S. Yamamoto, *et al.*, *Opt. Express* 29, 36353–36365 (2021)
- [23] Y. Ma, *et al.*, in *Proc. OFC19, M1A.3*, (2019).
- [24] T. Watanabe, *et al.*, in *Proc. OFC/NFOEC12*, pp. 1–3 (2012)
- [25] X. Ma, *et al.*, *IEEE Commun. Mag.*, 41, S16–S23, (2003)
- [26] T. Goh, *et al.*, in *Proc. OFC22*, paper W4B.1. (2022)
- [27] T. Kitoh, *et al.*, *IEEE Photon. Technol. Lett.*, 4, (1992)
- [28] K. Suzuki *et al.*, *J. Lightw. Technol.* 41, 3074–3083, (2023)